

FIRST-PRINCIPLES STUDY OF ISOMORPHIC ('DUAL-DEFECT') SUBSTITUTION IN KAOLINITE

MAN-CHAO HE¹, JIAN ZHAO^{1,*}, ZHI-JIE FANG¹, AND PING ZHANG²

¹ State Key Laboratory for Geomechanics and Deep Underground Engineering, China University of Mining and Technology, Beijing 100083, China

² Institute of Applied Physics and Computational Mathematics, Beijing 100088, China

Abstract—Kaolinite is often a cause of deformation in soft-rock tunnel engineering, leading to safety problems. In order to gain a better predictive understanding of the governing principles associated with this phenomenon, the physical and chemical properties of kaolinite were investigated using an efficient, first-principles scheme for studying isomorphic substitution of Al ions in kaolinite by two kinds of other elements (namely, the dual defect). Elements that are relatively common in natural kaolinite were chosen from groups II (Be, Mg, Ca, and Sr) and III (Fe and Sc) of the Periodic Table as dual-defect ions to substitute for Al ions in kaolinite. By systematically calculating the impurity-formation energies (which characterize the difference in the total crystal energy before and after the defect arises) and transition-energy levels, which characterize the energy cost for the transformation between two different charge states, the $(\text{Be} + \text{Sc})_{\text{Al}}$ (*i.e.* the replacement of two specific Al ions in kaolinite by external Be and Sc ions), $(\text{Ca} + \text{Sc})_{\text{Al}}$, $(\text{Mg} + \text{Sc})_{\text{Al}}$, and $(\text{Sr} + \text{Sc})_{\text{Al}}$ ion pairs were determined to have low formation energies, suggesting that these combinations of ions can easily substitute for Al ions in kaolinite. The $(\text{Be} + \text{Fe})_{\text{Al}}$, $(\text{Ca} + \text{Fe})_{\text{Al}}$, $(\text{Mg} + \text{Fe})_{\text{Al}}$, and $(\text{Sr} + \text{Fe})_{\text{Al}}$ ion pairs have relatively high formation energies which make isomorphic substitution (or doping) in kaolinite difficult. Moreover, these combinations of elements from groups II and III were found to have relatively low transition-energy levels compared with other element pairs. Among them, $(\text{Sr} + \text{Sc})_{\text{Al}}$ have the lowest transition-energy level at 0.06 eV above the valence band maximum. When compared with single external substitutional defects in kaolinite, remarkably, the dual defects have relatively low formation energies and transition-energy levels. The results are helpful in understanding the chemical and physical properties of natural kaolinite.

Key Words—First-principles Calculations, Engineering of Clays, Formation Energy, Kaolinite, Point Defect, Transition-energy Level.

INTRODUCTION

Dealing with large-scale deformations in soft-rock tunnels is a very important issue in soft-rock tunnel engineering. The mechanism of this large-scale deformation is closely related to the interaction between clay minerals and water molecules (He *et al.*, 2000, 2005). Kaolinite is one of the most abundant clay minerals, and so understanding the interaction between kaolinite and water molecules is important to those working in geophysics and geomechanics (Hu and Angelos, 2008). Understanding the physics and chemistry of kaolinite is the first step toward understanding this interaction. The stable crystal structure of ideal kaolinite, $\text{Al}_2\text{Si}_2\text{O}_5(\text{OH})_4$, with a perfect 1:1 layered structure consisting of two different surfaces (Adams, 1983; Teppen *et al.*, 1997), has been determined by numerous experimental measurements and theoretical calculations (Benco *et al.*, 2001; Bish, 1993; Giese, 1973; Hayashi, 1997; He *et al.*, 2009; Hess and Saunders, 1992; Hobbs *et al.*, 1997; Plançon *et al.*, 1997). However, various types of point defects may exist in kaolinite in the form

of atom or ion impurities in interstitial or interlayer sites, or replacing the normal lattice ions directly. Additional possibilities include lattice vacancies and polar defects (He *et al.*, 2009). In particular, when the substituent ion has a formal charge which is different from that of the replaced lattice ion, then the substitution defects may function as trapping sites for electrons (electron holes), which in turn provide adsorption centers for water molecules. The water molecules adsorbed on the clay surface or in the structure can reduce the mechanical strength of the clay minerals, leading to deformation of the rocks.

As natural kaolinite can have multiple defects, study of the physical and chemical properties of a kaolinite with two or more point defects is necessary. Experimentally, some substitution defects in natural and synthetic kaolinite, such as $\text{Fe}_{\text{Al}(\text{Si})}$ (which means the replacement of a specific Al or Si ion in kaolinite by an external Fe ion) and $(\text{Mg} + \text{Fe})_{\text{Al}(\text{Si})}$ (replacement of two specific Al or Si ions in kaolinite by external Mg and Fe ions) were investigated using electron spin resonance (ESR) measurements (Angel *et al.*, 1974; Poole and Farach, 1986). The ESR experimental measurements require full knowledge of the local structural and electronic properties of the defects, thus calling for an extensive first-principles study of kaolinite

* E-mail address of corresponding author:

zhaojian0209@yahoo.com.cn

DOI: 10.1346/CCMN.2011.0590507

with various kinds of substitution defects. Unlike the extensive *ab initio* studies (e.g. Hess and Saunders, 1992; Hobbs *et al.*, 1997) that have been carried out for pure kaolinite in the last decade, few theoretical works on defect-formation energies in kaolinite have been carried out (He *et al.*, 2009). To the authors' knowledge, no *ab initio* investigation of multiple-defects doping in kaolinite has been published. The present study reports a series of first-principles studies of kaolinite in which dual-defect formation energies and transition-energy levels that characterize the energy cost for the transformation between two different charge states were calculated. In the present study, elements from groups II (Be, Mg, Ca, and Sr) and III (Fe and Sc) were chosen as external ions to substitute for Al ions in kaolinite. In nature, the concentrations of the group-II elements Be, Mg, Ca, and Sr range from ~0.0015 to ~0.006%, ~1.33 to 4.64%, ~3.0 to ~8.08%, and ~0.13 to ~0.35% by weight, respectively. The concentrations of group-III elements Fe and Sc range from ~3.5 to ~8.24% and from ~0.0011 to ~0.0038% by weight, respectively (Chen and Wang, 2004). In the present study, the defects ranged in concentration from ~0.87 to 8.5% by weight, similar to those reported from other studies. The objective was to use a first-principles approach to help explain the various chemical and physical properties associated with multiple point defects in kaolinite from a microscopic perspective.

METHODS

Density-functional theory (DFT) using the local-density approximation (LDA) as implemented in the Vienna *ab initio* Simulation Package (VASP) (Kresse and Furthmüller, 1996) was applied to idealized kaolinite with the molecular formula $\text{Al}_2\text{Si}_2\text{O}_9\text{H}_4$ and space group *P1*. Projector augmented wave (PAW) pseudo-potentials (Blöchl, 1994; Kresse and Joubert, 1999) were used. All atomic positions were relaxed according to the calculated Hellmann-Feynman forces. The energy cutoff for the plane-wave basis was 400 eV, which is large enough to reduce the error from calculations of the formation energies and transition-energy levels to <0.01 eV. During calculations of dual-defect formation energies and defect transition-energy levels, the supercell approach was used in which a dual-defect α in charge state q was placed in a kaolinite supercell that was repeated periodically. All the calculations were performed using a $2 \times 2 \times 1$ supercell (containing 68 atoms). The defect system was modeled by arranging for a dual defect to substitute for two Al atoms at the center of a periodic supercell (Figure 1). The $2 \times 2 \times 1$ supercell was chosen to provide sufficient lattice sites to accommodate defect concentrations as low as 1.47 mol.%. For a charged defect, a uniform background charge was added to keep the global charge neutrality of the periodic supercell (Zhang *et al.*, 1997). The optimization

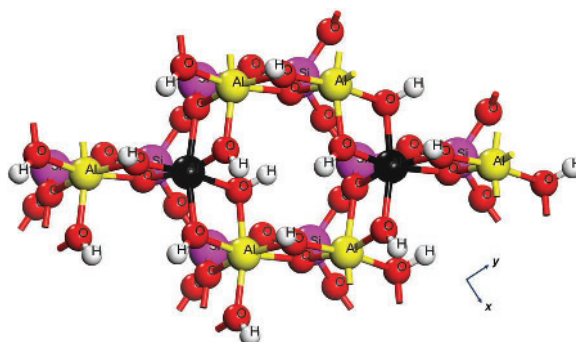


Figure 1. Top view of a dual defect replacing two Al ions at the center of a periodic supercell looking down the z axis. White spheres, red spheres, purple spheres, and dark yellow spheres represent hydrogen, oxygen, aluminum, and silicon, respectively. Black spheres represent the aluminum ions replaced by a dual defect.

of atomic geometries was performed *via* a conjugate-gradient algorithm until the residual forces acting on atoms were <0.01 eV/Å. The $2 \times 2 \times 2$ Monkhorst-Pack (Monkhorst and Pack, 1976) k -point set was used to sample the Brillouin zone. The calculated structural parameters $a = 5.160 \text{ \AA}$, $b = 5.160 \text{ \AA}$, $c = 7.602 \text{ \AA}$, $\alpha = 81^\circ$, $\beta = 89^\circ$, and $\gamma = 60.18^\circ$ were used throughout the study, in good agreement with experimental lattice parameters reported previously (Bish, 1993; Table 1).

By counting the number of valence electrons for the defect elements and host Al ions, one can predict, in principle, which of the doping elements will lead to a net negative charge. In kaolinite, substituting a group-II or group-III element for trivalent Al ions may introduce a corresponding net-negative charge. The valence electrons in kaolinite include 3s and 3p electrons of Al, 3s and 3p of Si, 1s of H, and 2s and 2p of O. For the group-II elements, the valence electrons include 2s of Be, 4s and 4p of Ca, 3s and 3p of Mg, and 5s and 5p of Sr. For the transition elements Fe and Sc the valence electrons include 3d and 4s, respectively. In order to determine which pairs of ions are the most stable in kaolinite, defect-formation energies and defect transition-energy levels were calculated for various types of dual defects. Following Wei and Zhang (2002), the dual-defect formation energy, $\Delta H_f(\alpha, q)$, as a function of the Fermi

Table 1. Calculated vs. experimental lattice parameters of kaolinite using basis sets were described in present study.

Phase	Calculated	Experimental	% Difference
a	5.160 Å	5.155 Å	0.9
b	5.160 Å	5.155 Å	0.9
c	7.602 Å	7.405 Å	2.5
α	81°	75.14°	7.2
β	89°	84.12°	5.4
γ	60.18°	60.18°	0

energy, E_F , and atomic chemical potential, μ_i , of the i th element were deduced. For the present system, $\Delta H_f(\alpha, q)$ is given by:

$$\Delta H_f(\alpha, q) = \Delta E(\alpha, q) + n_{\text{Al}}\mu_{\text{Al}} + n_{\text{Si}}\mu_{\text{Si}} + n_{\text{A}}\mu_{\text{A}} + n_{\text{O}}\mu_{\text{O}} + n_{\text{H}}\mu_{\text{H}} + qE_F \quad (1)$$

Here, $\Delta E(\alpha, q)$ can be determined by the following self-consistent total energy calculation:

$$\Delta E(\alpha, q) = E(\alpha, q) - E(\text{kaolinite}) + n_{\text{Al}}\mu_{\text{Al}}^0 + n_{\text{Si}}\mu_{\text{Si}}^0 + n_{\text{A}}\mu_{\text{A}}^0 + n_{\text{O}}\mu_{\text{O}}^0 + n_{\text{H}}\mu_{\text{H}}^0 + qE_{\text{VBM}} \quad (2)$$

$E(\alpha, q)$ is the total energy of the supercell containing the defect α in charge state q , $E(\text{kaolinite})$ is the total energy of the defect-free supercell containing 68 atoms, and n_{Al} , n_{Si} , n_{A} , n_{O} , and n_{H} are the number of Al, Si, external-defect (A), O, and H ions in the supercell, respectively. In the present case, the kaolinite keeps its equilibrium with bulk Al, Si, and doped ions under ambient conditions, therefore, μ_{Al}^0 , μ_{Si}^0 , and μ_{A}^0 are identical to the ground-state energies (per ion) of bulk Al (cubic close-packed), Si (diamond structure), and doped ions, *i.e.* $\mu_{\text{Al}}^0 = E_{\text{bulk}}(\text{Al})$, $\mu_{\text{Si}}^0 = E_{\text{bulk}}(\text{Si})$, and $\mu_{\text{A}}^0 = E_{\text{bulk}}(\text{A})$. Likewise, the chemical potentials μ_{H}^0 and μ_{O}^0

are given by half of the ground-state gas energies for hydrogen and oxygen molecules, respectively, *i.e.* $\mu_{\text{H}}^0 = 0.5E_{\text{H}_2}$ and $\mu_{\text{O}}^0 = 0.5E_{\text{O}_2}$. E_F in equation 1 is the Fermi energy measured from the valence band maximum (VBM), E_{VBM} . Depending on the experimental growth conditions, some thermodynamic limits exist for chemical potentials. In the present study, the chemical potential of kaolinite was not considered, *i.e.* all the results calculated were discussed for $\mu_i = 0$ in equation 1. The defect transition-energy level $\varepsilon_\alpha(q/q')$ is defined as the value of the Fermi level at which the formation energy of defect α in charge q is equal to that of defect α in q' :

$$\varepsilon\left(\frac{q}{q'}\right) = \frac{[\Delta E(\alpha, q) - \Delta E(\alpha, q')]}{q' - q} \quad (3)$$

According to the definition, $\varepsilon_\alpha(q/q')$ is independent of chemical potentials μ and the Fermi level E_F , and can be determined precisely from self-consistent calculations. The dual-defect transition levels of point defects referenced to the conduction band maximum (CBM) and VBM were calculated (Table 2).

Table 2. External dual defect formation energies in term of $\Delta E(\alpha, q)$ and defect transition levels $\varepsilon_\alpha(q/q')$ in kaolinite. n_{A} and n_{Al} are the numbers of doping atoms and Al atoms, and q are the numbers of excess electrons, transferred from the defect-free crystal to the reservoirs to form dual defects.

Defect α	$\Delta E(\alpha, q)$ (eV)	n_{A}	n_{Al}	q
$(\text{Be} + \text{Sc})_{\text{Al}}^0$	2.67	-2	2	0
$(\text{Be} + \text{Sc})_{\text{Al}}^-$	2.82	-2	2	-1
Defect transition level: $(-/0) = E_V + 0.15$ eV				
$(\text{Fe} + \text{Sc})_{\text{Al}}^0$	6.96	-2	2	0
$(\text{Fe} + \text{Sc})_{\text{Al}}^-$	7.39	-2	2	-1
Defect transition level: $(-/0) = E_V + 0.43$ eV				
$(\text{Ca} + \text{Sc})_{\text{Al}}^0$	2.46	-2	2	0
$(\text{Ca} + \text{Sc})_{\text{Al}}^-$	2.64	-2	2	-1
Defect transition level: $(-/0) = E_V + 0.08$ eV				
$(\text{Ca} + \text{Fe})_{\text{Al}}^0$	5.51	-2	2	0
$(\text{Ca} + \text{Fe})_{\text{Al}}^-$	5.94	-2	2	-1
Defect transition level: $(-/0) = E_V + 0.43$ eV				
$(\text{Mg} + \text{Sc})_{\text{Al}}^0$	1.48	-2	2	0
$(\text{Mg} + \text{Sc})_{\text{Al}}^-$	1.63	-2	2	-1
Defect transition level: $(-/0) = E_V + 0.15$ eV				
$(\text{Fe} + \text{Sc})_{\text{Al}}^0$	5.93	-2	2	0
$(\text{Fe} + \text{Sc})_{\text{Al}}^-$	6.35	-2	2	-1
Defect transition level: $(-/0) = E_V + 0.42$ eV				
$(\text{Sr} + \text{Sc})_{\text{Al}}^0$	1.38	-2	2	0
$(\text{Sr} + \text{Sc})_{\text{Al}}^-$	1.45	-2	2	-1
Defect transition level: $(-/0) = E_V + 0.06$ eV				
$(\text{Sr} + \text{Fe})_{\text{Al}}^0$	5.87	-2	2	0
$(\text{Sr} + \text{Fe})_{\text{Al}}^-$	6.42	-2	2	-1
Defect transition level: $(-/0) = E_V + 0.69$ eV				

RESULTS

The dual-defect formation energies, $\Delta H_f(\alpha, q)$, of each supercell in terms of $\Delta E(\alpha, q)$, n_{Al} , n_A , and q (as found in equation 2), as well as defect transition-energy levels $\varepsilon_\alpha(q/q')$ of equation 3 were calculated (Table 2). The valence states of the external ions in the present study are Be^{2+} , Ca^{2+} , Mg^{2+} , Sr^{2+} , Fe^{3+} , and Sc^{3+} . In the present study, focus was on the kind of external dual defects that can easily introduce charge-negative properties in kaolinite. From the calculated results, combining ions from groups II and III (Be, Ca, Mg, and Sr) with Sc, the formation energies $\Delta H_f(Be + Sc)_{Al}$, $\Delta H_f(Ca + Sc)_{Al}$, $\Delta H_f(Mg + Sc)_{Al}$, and $\Delta H_f(Sr + Sc)_{Al}$ for $q = 0$ were 2.67, 2.46, 1.48, and 1.38 eV, respectively.

Of the ions in groups II and III, Sr and Sc are the most promising dual-doping ions which substitute for Al ions because they have the lowest formation energy. In addition, considering the transition-energy level position, $(Sr + Sc)_{Al}$ has a relatively low transition-energy level $\varepsilon(-1/0)$, 0.06 eV above the VBM. A high transition-energy level indicates that this kind of defect would not easily introduce negative charge, while a low level indicates the opposite. In the present system, one concern is to determine which kinds of dual defects can easily introduce negative-charge properties. From the results, $(Sr + Sc)$ ions that substitute for Al ions can easily introduce negative charge, because $(Sr + Sc)_{Al}$ has the lowest transition-energy level.

For the combination of Be, Ca, Mg, and Sr with Fe, the formation energies $\Delta H_f(Be + Fe)_{Al}$, $\Delta H_f(Ca + Fe)_{Al}$, $\Delta H_f(Mg + Fe)_{Al}$, and $\Delta H_f(Sr + Fe)_{Al}$ are 6.93, 5.51, 5.93, and 5.87 eV, respectively. These kinds of dual defects have relatively high formation energies compared with Sc-coupled defects, which means that these defects are more difficult to form than the combinations

above. However, the transition-energy levels of $(Be + Fe)_{Al}$, $(Ca + Fe)_{Al}$, $(Mg + Fe)_{Al}$, and $(Sr + Fe)_{Al}$ are 0.43, 0.43, 0.42, and 0.55 eV, respectively, above the VBM (low defect levels with localized electronic states). Other dual-defect combinations of groups II and III elements were also tested. The results revealed that the formation energies and transition-energy levels were even higher. Thus, those dual defects would be very unlikely to be doped in Al ion sites and so difficult to form. If they were to form, no observable change in negative charge in kaolinite would be introduced.

The formation energies of the various kinds of external substitutional defects vs. the Fermi energy E_F (Figure 2) revealed that E_F is bounded between E_{VBM} and E_{CBM} , the difference between which gives the insulating band gap. The calculated band gap is 4.89 eV. When the Fermi level, E_F , moves toward the CBM, according to equation 1, the formation energy of external defects will decrease. In the case of $(Sr + Sc)_{Al}$, when E_F is located at VBM, the formation energy $\Delta H_f(Sr + Sc)_{Al} = 1.38$ eV, which means that the $(Sr + Sc)_{Al}$ dual defect is easy to form and its formation energy $\Delta H_f(Sr + Sc)_{Al}$ decreases with increase in the Fermi level. As the value of E_F approaches 1.45 eV, the formation energy of $(Sr + Sc)_{Al}$ becomes negative, revealing that the dual defect $(Sr + Sc)_{Al}$ can be formed spontaneously when $E_F > 1.45$ eV. The formation energies for $\Delta H_f(Ca + Sc)_{Al}$, $\Delta H_f(Mg + Sc)_{Al}$, and $\Delta H_f(Be + Sc)_{Al}$ (Figure 3) also became negative when E_F reached 2.64, 1.63, and 2.82 eV, respectively. Only the formation energies $\Delta H_f(Be + Fe)_{Al}$, $\Delta H_f(Ca + Fe)_{Al}$, $\Delta H_f(Mg + Fe)_{Al}$, and $\Delta H_f(Sr + Fe)_{Al}$ were always positive within the energy gap. This result implies that these atoms are very difficult to substitute into kaolinite.

Plots (Figure 3) were made of the orbital-resolved site-projected density of states (PDOS) for Be, Fe, O,

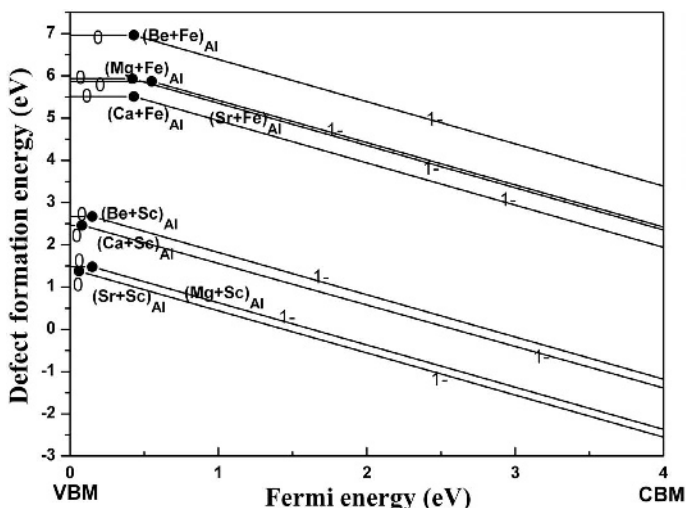


Figure 2. Formation energies (equation 1) vs. the Fermi energy for replaced defects in kaolinite. The charge state q determines the slope of each line segment.

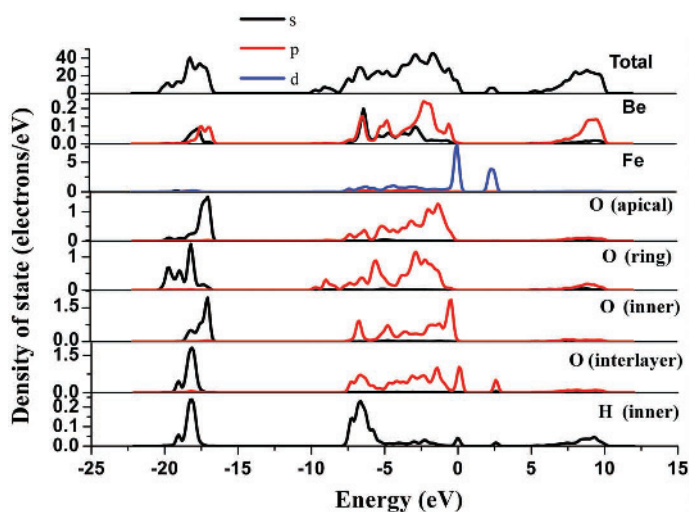


Figure 3. Orbital-resolved partial DOS for Be, Fe, O, and H atoms (from top to bottom) in a kaolinite unit cell. The Fermi energy is set at zero. The total DOS is also plotted along the top.

and H atoms (one atom for each atomic component) in a single kaolinite unit cell, with the Fermi energy set to zero. The PDOS of the four different kinds of oxygen atoms, which were similar to each other, were plotted separately because of their different symmetries and positions in the unit cell. This similarity is due to the high electronegativity of oxygen, which results in a large charge transfer from the Be 2s, Fe 3d, and H 1p states to the O 2p states. In fact, the valence bands in a wide energy range ($-10\text{eV} < E < E_F$) are largely composed of O 2p states (Figure 3). On the other hand, some residual charges are also to be found in the Be 2s/2p and Fe 4s/3d states, implying that an observable covalent component also exists in the Be–O and Fe–O chemical bonds in the kaolinite (Figure 3).

To obtain a more precise understanding of the different kinds of dual defect in kaolinite, the crystal charge-density distribution maps of $(\text{Mg} + \text{Fe})_{\text{Al}}$ were plotted (Figure 4). Observable covalent bonding between Fe and O in kaolinite was noted (Figure 4a), which implies that no residual charges occur in kaolinite. As no similar covalent component between Mg and O was observed, Mg-doping can clearly accommodate the negative charge in kaolinite more easily. Counting the number of valence electrons of the dopants and the host element could lead to the negative charge. When divalent elements of groups II and III replace the trivalent Al ions, a net-negative charge is introduced. If the transition elements become trivalent cations in kaolinite, however, maintaining the negative charges becomes difficult.

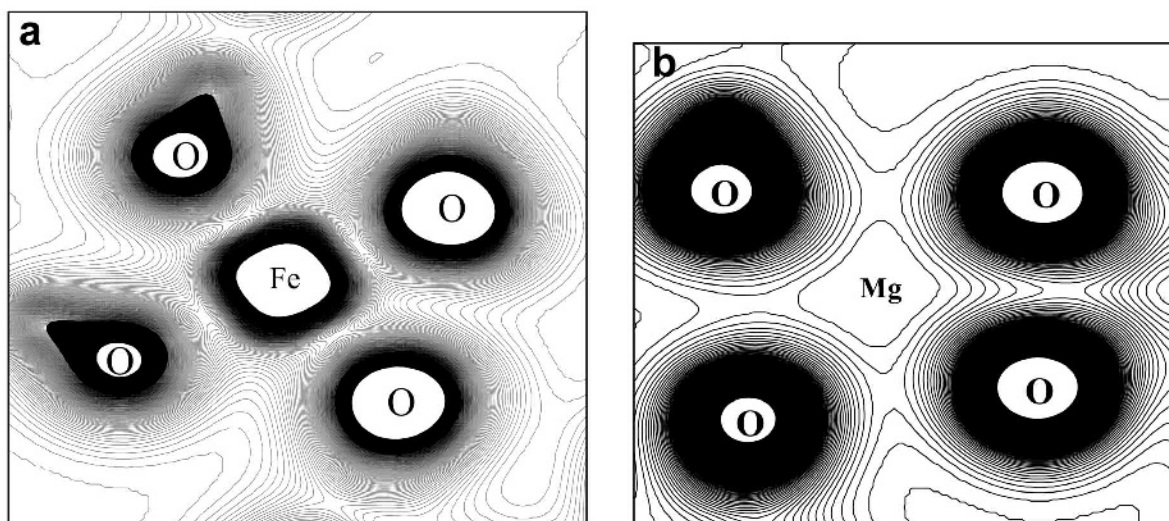


Figure 4. Charge-density distributions for kaolinite with dual-defect Fe (a) and Mg (b) included. The plot plane is fixed by one defect atom and two apical oxygen atoms which bridge the silicon-ring system to the Al layers.

SUMMARY

External dual defects in kaolinite were studied using first-principles DFT-LDA calculations. All combinations of group-II and group-III elements as dual-defect dopants had relatively low transition-energy levels. $(\text{Sr} + \text{Sc})_{\text{Al}}$ gave the lowest transition-energy level at 0.06 eV above the VBM, which means that $(\text{Sr} + \text{Sc})_{\text{Al}}$ can accommodate negative charge in kaolinite. $(\text{Be} + \text{Sc})_{\text{Al}}$, $(\text{Ca} + \text{Sc})_{\text{Al}}$, $(\text{Mg} + \text{Sc})_{\text{Al}}$, and $(\text{Sr} + \text{Sc})_{\text{Al}}$ have low formation energies, suggesting that they can easily substitute for Al ions. $(\text{Be} + \text{Fe})_{\text{Al}}$, $(\text{Ca} + \text{Fe})_{\text{Al}}$, $(\text{Mg} + \text{Fe})_{\text{Al}}$, and $(\text{Sr} + \text{Fe})_{\text{Al}}$ have relatively high formation energies and so will not be accommodated easily in kaolinite, nor can they supply much negative charge. Compared with previous research on single external substitutional defects in kaolinite, external dual defects in kaolinite had relatively low formation energies and transition-energy levels, meaning that dual defects will form more easily and introduce negative-charge properties. The present research on multiple-point defects in kaolinite is close to the situation found in natural kaolinite in engineering environments.

ACKNOWLEDGMENTS

This research was supported by the state 973 project (No. 2006CB202200), the Program for Changjiang Scholars and Innovative Research Team in University of China under Grant No. IRT0656, and the National Natural Science Foundation of China (No. 40972196).

REFERENCES

- Adams, J.M. (1983) Hydrogen atom position in kaolinite by neutron profile refinement. *Clays and Clay Minerals*, **31**, 352–358.
- Angel, B.R., Jones, J.P.E., and Hall, P.L. (1974) Electron spin resonance studies of doped synthetic kaolinites. *Clays and Clay Minerals*, **10**, 247–255.
- Benco, L., Tunega, D., Hafner, J., and Lischka, H. (2001) Orientation of OH groups in kaolinite and dickite: *ab initio* molecular dynamics study. *American Mineralogist*, **86**, 1057–1065.
- Bish, D.L. (1993) Rietveld refinement of the kaolinite structure at 1.5 K. *Clays and Clay Minerals*, **41**, 738–744.
- Blöchl, P.E. (1994) Projector augmented-wave method. *Physical Review B*, **50**, 17953–17979.
- Chen, J. and Wang, H.N. (2004) Pp. 35–60 in: *Geochemistry*. (H.Y. Xie and P. Liu, editors). Science Press, Beijing.
- Giese, R.F., JR. (1973) Interlayer bonding in kaolinite dickite and nacrite. *Clays and Clay Minerals*, **21**, 145–149.
- Hayashi, S. (1997) NMR study of dynamics and evolution of guest molecules in kaolinite/dimethyl sulfoxide intercalation compound. *Clays and Clay Minerals*, **45**, 724–732.
- He, M.C., Jing, H.H., and Yao, A.J. (2000) Research progress of soft rock engineering geomechanics in China coal mine. *Journal of Engineering Geology*, **1**, 46–62.
- He, M.C., Xie, H.P., and Peng, S.P. (2005) Study on rock mechanics in deep mining engineering. *Chinese Journal of Rock Mechanics and Engineering*, **24**, 2803–2813.
- He, M.C., Fang, Z.J., and Zhang, P. (2009) Theoretical studies on the defects of kaolinite in clays. *Chinese Physics Letter*, **26**, 059101–059104.
- Hess, A.C. and Saunders, V.R. (1992) Periodic *ab initio* Hartree-Fock calculation of the low-symmetry mineral kaolinite. *The Journal of Physical Chemistry*, **11**, 4367–4374.
- Hobbs, J.D., Cygan, R.T., Nagy, K.L., Schultz, P.A., and Sears, M.P. (1997) All-atom *ab initio* energy minimization of the kaolinite crystal structure. *American Mineralogist*, **82**, 657–662.
- Hu, X.L. and Angelos, M. (2008) Water on the hydroxylated (001) surface of kaolinite: From monomer adsorption to a flat 2D wetting layer. *Surface Science*, **602**, 960–974.
- Kresse, G. and Furthmüller, J. (1996) Efficient iterative schemes for *ab initio* total-energy calculations using a plane-wave basis set. *Physical Review B*, **54**, 11169–11186.
- Kresse, G. and Joubert, J. (1999) From ultrasoft pseudopotentials to the projector augmented-wave method. *Physical Review B*, **59**, 1758–1762.
- Monkhorst, H.J. and Pack, J.D. (1976) Special points for Brillouin-zone integrations. *Physical Review B*, **13**, 5188–5192.
- Plançon, A., Giese, R.F. Jr., Snyder, R., Drits, V.A., and Bookin, A.S. (1997) Stacking faults in the kaolinite-group minerals: defect structures of kaolinite. *Clays and Clay Minerals*, **37**, 195–198.
- Poole, C.P. Jr. and Farach, H.A. (1986) Electron spin resonance. *ASM Handbook*, **10**, 253–266.
- Teppen, B.J., Rasmussen, K., Bertsch, P.M., Miller, D.M., and Schäferll, L. (1997) Molecular dynamic modeling of clay minerals. 1. Gibbsite, kaolinite, pyrophyllite, and beidellite. *The Journal of Physical Chemistry B*, **101**, 1579–1587.
- Wei, S.H. and Zhang, S.B. (2002) Chemical trends of defect formation and doping limit in II-VI semiconductors: The case of CdTe. *Physical Review B*, **66**, 155211–155221.
- Zhang, S.B., Wei, S.H., and Zunger, A. (1997) Stabilization of ternary compounds via ordered arrays of defect pairs. *Physical Review Letter*, **78**, 4059–4062.

(Received 24 August 2010; revised 3 October 2011; Ms. 478; A.E. H. Dong)